Reaction of EDTA and Related Aminocarboxylate Chelating Agents with Co^{III}OOH (Heterogenite) and Mn^{III}OOH (Manganite)

C H R I S T A   S.   M C A R D E L L,[†]
A L A N   T.   S T O N E,* A N D   J I A H E R   T I A N

Department of Geography and Environmental Engineering,
The Johns Hopkins University, Baltimore, Maryland 21218

AAS and capillary electrophoresis have been used to identify dissolved products of the reaction of EDTA, NTA, and related aminocarboxylate chelating agents with CoOOH (heterogenite), representing the sorbed contaminant metal Co^{III}, and MnOOH (manganite), representing the naturally occurring metal Mn^{III}. Reaction of CoOOH with EDTA and NTA yields both ligand-assisted dissolution products (i.e., dissolved Co^{III} species) and reductive dissolution products (Co^{II} and chelating agent products of oxidative dealkylation). Reaction of CoOOH with IDA yields only ligand-assisted dissolution products. Reaction of MnOOH with all aminocarboxylates examined (EDTA, HEEDTA, NTA, and IDA) yields reductive dissolution products only; dissolved Mn^{III} complexes are not detected. These findings improve our understanding of co-contaminant reactions affecting the subsurface behavior of chelating agents, metallic elements, and radionuclides.

Introduction

Past disposal activities, now curtailed, released synthetic aminocarboxylate chelating agents (e.g., EDTA and NTA) and radioactive cobalt-60 into shallow landfills (*1–3*). One site at Oak Ridge, TN, has generated a cobalt- and EDTA-containing plume that has migrated several kilometers away from the disposal site (*4*). Co^{III}EDTA$^-$, which has been tentatively identified in this plume, sorbs poorly onto aquifer solids (*5–7*) and appears resistant to chemical and biological degradation. NTA and other aminocarboxylate chelating agents (e.g., breakdown products of EDTA) may also be capable of solubilizing cobalt, facilitating its movement in the hydrologic cycle, and providing a route of exposure to humans and other organisms. For these reasons, it is important to quantify source and sink terms for dissolved Co^{III} complexes.

Two pathways for the formation of Co^{III}EDTA$^-$ can be envisioned. In the first pathway, Co^{II} and EDTA form the complex Co^{II}EDTA^{2-}, which is subsequently oxidized to Co^{III}EDTA$^-$. Flow column experiments have established that MnO$_2$ (*8*) and Fe(OH)$_3$ (*9*) can oxidize Co^{II}EDTA^{2-} to Co^{III}EDTA$^-$. In the second pathway, oxidation of Co^{II} to Co^{III} occurs prior to complex formation with EDTA. X-ray photoelectron spectroscopy has established that Co^{II} ad-

sorbed onto manganese(III,IV) and iron(III) (hydr)oxides is slowly oxidized to Co^{III} (*10–12*). Ligand-assisted dissolution of adsorbed or precipitated Co^{III}, however, has not been previously investigated.

In addition to the ligand-assisted dissolution reaction just described, oxidation of EDTA by Co^{III} may also take place. Using the mineral phase CoOOH (heterogenite) as a representative Co^{III}-containing phase, the following half-reaction can be written:

$$CoOOH + 3H^+ + e^- = Co^{2+} + 2H_2O$$

$$E^\circ = 1.48 \text{ V } (13) \quad (1)$$
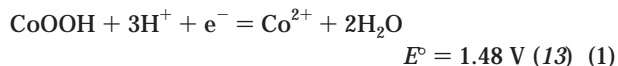
For comparison, $E^\circ = 1.50$ V for the MnOOH (manganite)/Mn^{2+} half-reaction (*14*) and $E^\circ = +0.67$ V for the FeOOH (goethite)/Fe^{2+} half-reaction (*15*). Thus, CoOOH nearly matches the thermodynamic oxidant strength of MnOOH, known from previous studies to oxidize EDTA (*16*).

Monitoring reactions of EDTA with the mixed manganese, iron, and cobalt (hydr)oxides found in soils and sediments is inherently difficult. EDTA, EDTA oxidation products, and their complexes with Mn^{II}, Mn^{III}, Fe^{II}, Fe^{III}, Co^{II}, and Co^{III} are all potentially important participants; metal-to-metal electron transfer, ligand exchange, and metal ion exchange reactions all play a role in determining product distribution. As noted by Klewicki and Morgan (*16*), reactions of aminocarboxylates with Mn and Fe (hydr)oxides are important for a variety of reasons, even when contaminant metal ions are absent.

The present work investigates the reactions of EDTA and related aminocarboxylate chelating agents with Co^{III}OOH (heterogenite) and Mn^{III}OOH (manganite). Both (hydr)oxides can be prepared in nearly stoichiometric form. Appearance of Co^{II} or Mn^{II} in the reaction medium can therefore be used as proof that reductive dissolution has taken place. Using capillary electrophoresis techniques described in our previous paper (*17*), free aminocarboxylate chelating agents, their oxidation products, and in many instances their metal ion complexes can be resolved from one another and quantified. (Structures for all aminocarboxylates mentioned in this work are shown in Figure 1.) The principal objectives of this work are to identify reaction intermediates and products and to explore factors affecting yield.

An Overview of Possible Reaction Pathways. Figure 2 presents 11 distinct reaction pathways that may play a role in the reaction of EDTA with CoOOH. The parent compound EDTA exists in one or more different protonation levels prior to complexation by Co^{II} and Co^{III}. (EDTA)$_{oxidized}$ represents a potentially long list of possible EDTA oxidation products. One possible oxidation product, ED3A, is used to illustrate possible ligand exchange reactions.

Adsorption is the basis for all surface chemical reactions (e.g., reaction 1). Free EDTA, free oxidation products, free metal ions, metal ion–EDTA complexes, and metal ion–oxidation product complexes may all adsorb to some degree; adsorption affects all other reactions and interferes with efforts to monitor reaction progress.

The first block (Figure 2) represents reactions of free, uncomplexed EDTA with CoOOH. EDTA may extract Co^{III} from the surface, yielding Co^{III}EDTA$^-$ (reaction 2). Ligand-assisted dissolution does not involve electron transfer. Alternatively, EDTA may serve as a reductant toward the surface, resulting in the production of Co^{II} and EDTA oxidation products such as ED3A (reaction 3). Co^{II} may exist as an adsorbed species, as a "free" species in solution, or as a complex with EDTA or its oxidation products.

The second block represents homogeneous phase reactions that involve dissolved cobalt species generated by the first

* Corresponding author phone: (410) 516-8476; fax: (410) 516-8996; e-mail: astone@jhu.edu.
[†] Present address: Swiss Federal Institute for Environmental Science and Technology (EAWAG), CH-8600 Dübendorf, Switzerland. E-mail: mcardell@eawag.ch.
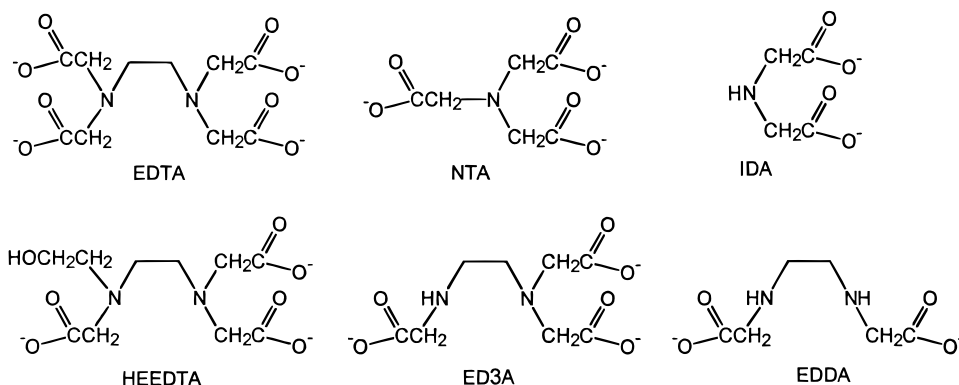
FIGURE 1. Structures of aminocarboxylate chelating agents mentioned in the text.
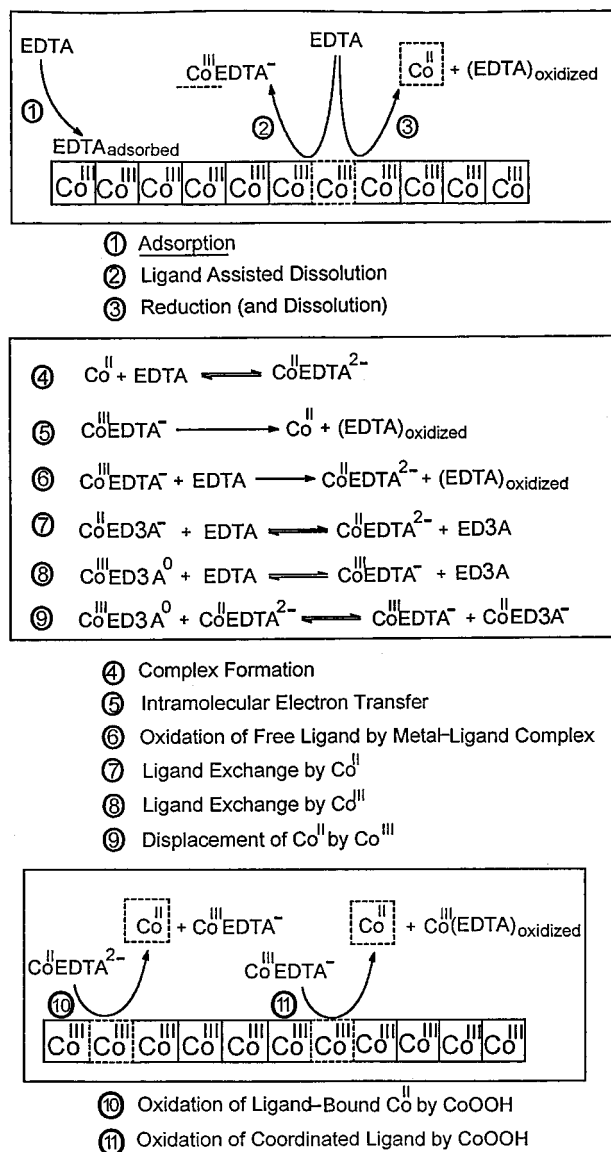
EDTA   NTA   IDA

HEEDTA   ED3A   EDDA

EDTA

① Adsorption

EDTA_adsorbed

Co^{III}EDTA$^-$ $\boxed{Co^{II}}$ + (EDTA)$_{oxidized}$

② ③

① Adsorption
② Ligand Assisted Dissolution
③ Reduction (and Dissolution)

④ Co^{II} + EDTA $\rightleftharpoons$ Co^{II}EDTA^{2-}

⑤ Co^{III}EDTA$^-$ $\longrightarrow$ Co^{II} + (EDTA)$_{oxidized}$

⑥ Co^{III}EDTA$^-$ + EDTA $\longrightarrow$ Co^{II}EDTA^{2-} + (EDTA)$_{oxidized}$

⑦ Co^{II}ED3A$^-$ + EDTA $\rightleftharpoons$ Co^{II}EDTA^{2-} + ED3A

⑧ Co^{III}ED3A^0 + EDTA $\rightleftharpoons$ Co^{III}EDTA$^-$ + ED3A

⑨ Co^{III}ED3A^0 + Co^{II}EDTA^{2-} $\rightleftharpoons$ Co^{III}EDTA$^-$ + Co^{II}ED3A$^-$

④ Complex Formation
⑤ Intramolecular Electron Transfer
⑥ Oxidation of Free Ligand by Metal–Ligand Complex
⑦ Ligand Exchange by Co^{II}
⑧ Ligand Exchange by Co^{III}
⑨ Displacement of Co^{II} by Co^{III}

$\boxed{Co^{II}}$ + Co^{III}EDTA$^-$ $\boxed{Co^{II}}$ + Co^{III}(EDTA)$_{oxidized}$

Co^{II}EDTA^{2-} Co^{III}EDTA$^-$

⑩ ⑪

⑩ Oxidation of Ligand–Bound Co^{II} by CoOOH
⑪ Oxidation of Coordinated Ligand by CoOOH

FIGURE 2. Possible pathways for reaction of EDTA with CoOOH.

block of reactions. Free EDTA is capable of complexing free metal ions (reaction 4) or of displacing lower-denticity oxidation products (reactions 7 and 8) via ligand exchange. Metal ion exchange reactions (reaction 9) are driven by log K differences (log K values for Co^{III}–aminocarboxylate complexes are larger than for analogous Co^{II} complexes) or by concentration differences (in principle, Co^{II} at sufficiently high concentrations can displace Co^{III}). The second block

also includes electron-transfer reactions: intramolecular oxidation of coordinated ligand by Co^{III} (reaction 5) and bimolecular oxidation of free ligand by Co^{III}–ligand complexes (reaction 6).

The third block illustrates reactions of dissolved Co^{II} and Co^{III} complexes with the CoOOH surface. Reaction 10 represents electron transfer from Co^{II}EDTA^{2-} to Co^{III} atoms residing within the CoOOH surface. If reaction 10 is fast relative to reactions 1 and 2, autocatalytic dissolution will be observed: buildup of Co^{II}EDTA^{2-} causes dissolution rates to increase as the reaction progresses. In reaction 11, Co^{III} within the CoOOH surface oxidizes EDTA coordinated to Co^{III} in solution. Reactions analogous to reactions 1–9 can also be postulated for other aminocarboxylate chelating agents and for reactions involving MnOOH.

Information Regarding Ligand Exchange. Ligand exchange involving +II metal ions (reactions 4 and 7) are inherently faster than those involving +III metal ions (reactions 2, 8, and 9). In comparison to other +III metal ions, Mn^{III} generally exhibits high rates of ligand exchange (arising from Jahn–Teller distortion), whereas Co^{III} exhibits exceptionally low rates of ligand exchange (arising from its low-spin electronic configuration and highest possible crystal field stabilization energy) (*18*).

Information Regarding Electron Transfer. Intramolecular ligand-to-metal electron transfer (reaction 5) occurs on time scales greater than 2 weeks for most Co^{III}–aminocarboxylate complexes. In contrast, the half-life for intramolecular electron transfer is 16 h for Mn^{III}EDTA$^-$ (3 < pH < 6) and 4.6 h for Mn^{III}HEEDTA^0 (4 < pH < 7) (*19*).

Oxidation of free aminocarboxylate ions by Mn^{III}–aminocarboxylate complexes (reaction 6) occurs more rapidly than intramolecular ligand-to-metal electron transfer. EDTA, NTA, and IDA oxidation by Mn^{III}CDTA$^-$, for example, is more rapid than intramolecular electron transfer within the Mn^{III}CDTA$^-$ complex (*20*). Reaction rates are proportional to free aminocarboxylate concentrations and are diminished when complexation by redox-active (e.g., Mn^{II}) or redox-inert (e.g., Zn^{II}) metal ions occurs (*20*). Indeed, Klewicki and Morgan (*16*) noted that Mn^{III}EDTA$^-$ decomposition rates increase substantially when free EDTA concentrations are increased. By analogy, oxidation of free aminocarboxylate ions by Co^{III}–aminocarboxylate complexes should also occur more rapidly than intramolecular ligand-to-metal electron transfer.

Reaction 10 is driven by the lower reduction potential for the Co^{III}EDTA$^-$/Co^{II}EDTA^{2-} half-reaction ($E^\circ = +0.47$ V) in comparison to that of the CoOOH/Co^{2+} half-reaction ($E^\circ = +1.48$ V). This also applies to the analogous Mn cross-reaction.

Ligand oxidation via a pathway analogous to reaction 11 has been reported. Co^{III}EDTA$^-$(aq) is oxidized to Co^{III}ED3A^0-(aq) by PbO$_2$(s) (*21*). The reaction is highly selective (81%

yield), and no further oxidation occurs. The authors hypothesized that coordination of EDTA to Co[III] results in three sterically distorted five-membered chelate rings; oxidation to ED3A lessens this steric strain.

Oxidation of aminocarboxylates by +III metal oxidants typically occurs via N-dealkylation. If the first oxidation step involves loss of an electron from an amine group, then glyoxylate should also appear as an oxidation product (e.g., ref 22). If the first step involves loss of an electron from the carboxylate group, inorganic carbonate and formaldehyde should also appear as oxidation products (e.g., ref 20). Regardless of which mechanism predominates, stoichiometric considerations indicate that 2 mol of +III metal ions should be reduced for each oxidative N-dealkylation.

Materials and Methods

Chemicals. All solutions and suspensions were prepared from distilled, deionized water (DDW, Millipore Corp., MA). All laboratory ware was cleaned in 5 M HNO_3 and rinsed several times with DDW prior to use. Analytical grade chemicals were used without additional purification.

Aminocarboxylic acids, except otherwise noted, were purchased from Aldrich. EDMA (ethylenediaminemonoacetic acid) was purchased from TCI America, and OX (oxalic acid) was from Baker Chemical Co. ED3A was synthesized in Battelle Pacific Northwest Laboratories (Richland, WA). $Co^{II}Cl_2 \cdot 6H_2O$ and $Mn^{II}Cl_2 \cdot 4H_2O$, both purchased from Baker Chemical Co., were used to prepare stock solutions of +II metal ions. Stock solutions containing metal chloride salts and aminocarboxylic acids were mixed at least 24 h prior to analysis to ensure equilibration.

As described in our previous paper (17), $Co^{III}EDTA^-$ (23), $u\text{-}fac\text{-}Co^{III}(IDA)_2^-$, and $s\text{-}fac\text{-}Co^{III}(IDA)_2^-$ (24) were synthesized by oxidizing Co^{II} complexes of the appropriate aminocarboxylate with H_2O_2. $Co^{III}ED3A^0$ was synthesized according to procedures outlined in ref 21. Three Co^{III} complexes with NTA were synthesized. A first product, most probably an oxo- or hydroxo-bridged dimer, is transformed by heating or acidification with acetic acid into another complex, probably the $Co^{III}NTA(OH)^-$ monomer (see ref 17). We will refer to this monomer complex as $(Co^{III}NTA)_1$. A third complex synthesized according to Mori et al. (25) corresponds to a hydroxo-bridged dimer, which we will refer to as $(Co^{III}NTA)_2$.

Preparation of CoOOH and MnOOH. CoOOH was synthesized by precipitating cobalt(II) hydroxide before adding the oxidant NaOCl. The 3 L of DDW at 80 °C was sparged with inert gas for 1 h before 100 mL of 0.71 M NaOH was added. One hour later, 80 mL of 0.228 M $CoCl_2$ (sparged for 90 min) was added under inert gas. Twenty minutes later, 50 mL of 0.74 M NaOCl was added under constant stirring. For the next 6 h, the suspension was kept at 80 °C, and more NaOCl was added, for a total of 250 mL. The oxide suspension was placed in an oven for 62 h at 80−85 °C. A washing procedure using centrifugation to collect the particles and sonication to resuspend the particles in fresh DDW was repeated seven times. At this point, the supernatant solution exhibited a specific conductance less than that of a 0.1 mM NaCl solution. CoOOH was stored in suspension. Dissolved Co in the supernatant solution was less than 3 μM, the detection limit of flame atomic absorption spectrophotometry (AAS).

Powder X-ray diffraction (XRD) yields sharp diffraction lines with d spacings corresponding to 4.29, 2.46, 2.32, 1.82, 1.43, 1.36, and 0.88 Å, indicating that the preparation contains the CoOOH mineral heterogenite in a relatively crystalline form (26, 27). Total cobalt was determined by AAS after complete reductive dissolution of the particle suspension by hydroquinone in HNO_3. Oxidizing titer of oxide particles was determined by measuring remaining hydroquinone and

its sole oxidation product p-benzoquinone with reversed-phase HPLC (u-Bondapak-C_{18} column, Waters Corp.) with UV detection. An average cobalt oxidation state of +3.02 ± 0.07 was found, close to the stoichiometry of CoOOH. Transmission electron microscopy (TEM) indicates that the sample consists of between 80 and 190 nm wide thin hexagonal plates.

The experiments with NTA employed a CoOOH sample prepared by a slightly different procedure. NaOH and NaOCl were added simultaneously to an argon-sparged Co^{II} solution; the resulting suspension was heated in an autoclave for 16 h at 120 °C. Following washing, XRD and TEM indicated that the preparation contains smaller (less than 20 nm), poorly crystalline heterogenite. The two CoOOH samples were compared in a limited number of dissolution experiments; no significant difference in reaction product distribution was observed.

MnOOH was synthesized following a modification of the method of Giovanoli and Leuenberger (28). Heating of a 2-L 6.0×10^{-2} M $MnSO_4$ solution to 60 °C was followed by the addition of 41 mL of 8.8 M H_2O_2 and subsequent slow addition of 600 mL of 0.20 M NH_4OH. (All three solutions were sparged with N_2 before and after mixing.) The resulting brown suspension was quickly heated to 95 °C; this temperature was maintained during stirring for 6 h. After overnight cooling, the suspension was washed 10 times using the centrifugation/sonication technique described for CoOOH.

An average manganese oxidation state of +3.0 was determined by AAS and by oxalate/$KMnO_4$ titration (method of McBride, as described by ref 29). TEM revealed fine needles that are approximately 400 nm long and 23 nm wide. d spacings measured by electron diffraction (3.10, 2.86, 2.63, 2.49, 2.39, 2.19, 1.77, and 1.64 Å) are consistent with the mineral manganite (30).

Capillary Electrophoresis Analysis. Details regarding the use of capillary electrophoresis (CE) for identifying and quantifying free aminocarboxylates and their Co^{II} and Co^{III} complexes are provided in our earlier paper (17). Mn^{II} and Mn^{III} complexes were analyzed using the same procedures. A Quanta 4000E CE instrument (Waters, Milford, MA) was used. Bare fused silica capillaries of 75 μm diameter and 60 cm length to the detector (68 cm total length) were used (Polymicro Technologies, Phoenix, AZ). The carrier electrolyte consisted of 25 mM phosphate buffer (pH = 7) and 0.5 mM tetradecyltrimethylammonium bromide (TTAB, Aldrich) electroosmotic flow modifier. Direct UV photometric detection at 185 nm and hydrostatic injection at 10 cm for 30 s were used at a run current of 50 μA and with a negative power supply at 25 °C constant temperature. Some CE runs were repeated at 254 nm. The capillary was flushed between samples with 0.1 M KOH followed by distilled water to wash out residual ions.

Several conclusions drawn from our earlier work (17) regarding peak identification are pertinent here: (i) Co^{III}−aminocarboxylate complexes absorb more strongly at 254 nm than at 185 nm. The same should also hold for Mn^{III} complexes. (ii) All Co^{III}−aminocarboxylate complexes prepared in our laboratory yield linear calibration plots and hence readily quantifiable peaks. Mn^{III} complexes with EDTA, NTA, and other polydentate aminocarboxylates should behave in the same way. (iii) Co^{II}−aminocarboxylate complexes absorb less at 254 nm than at 185 nm but are still visible. Mn^{II} complexes are transparent at 254 nm. (iv) Although Co^{II} complexes with EDTA and HEEDTA yield linear plots, those with NTA and with aminocarboxylates with log K values lower than those of NTA pose quantification difficulties. Mn^{II}−aminocarboxylate complexes also yield quantification difficulties. The detection limit for the N-dealkylation product glyoxylate is 20 μM (17); carbonate and formaldehyde cannot be detected by our technique.

The pH buffers employed in the present work electromigrate and yield broad peaks that can hide smaller peaks derived from reaction intermediates and products. To discern all CE peaks, duplicate experiments were performed with additional buffers whose corresponding anions electromigrate at substantially different rates: benzoate was substituted for acetate, and MOPS was substituted for HEPES.

Experimental Design. Product yield as a function of time was monitored in Teflon beakers immersed in a 25.0 ± 0.5 °C constant-temperature bath and covered with polypropylene plates. Constant pH was maintained using acetate, benzoate, HEPES, or MOPS buffers (chemicals from Aldrich). Suspension pH was measured using a glass electrode (Orion) calibrated against Orion standard buffer solutions. Suspensions were sparged with argon for 1 h prior to aminocarboxylate addition to keep dissolved O_2 and CO_2 to a minimum. The $5-10$-mL aliquots of reaction suspension were collected at specified time intervals and filtered through 0.1 μm pore diameter polycarbonate filters (Nuclepore Corp). Supernatant solution was analyzed directly by CE or acidified using HNO_3 in preparation for AAS analysis.

Product yield as a function of EDTA, NTA, and IDA concentration was measured in a series of amber glass vials sealed with silicon rubber septa immersed in a 25.0 ± 0.5 °C constant-temperature bath. No argon sparging was used. Acetate, benzoate, HEPES, or MOPS buffers were again employed. In some experiments, $NaNO_3$ (Baker) was added to ensure a final ionic strength of 0.01 M. No significant difference was observed between experiments performed with and without $NaNO_3$ additions. Unless otherwise stated, all reactors were filtered and analyzed at the same time. This time was selected based upon results of earlier experiments to ensure that reaction products had reached their final values. Plate counts were performed in a limited number of experiments to confirm the absence of bacteria. Addition of the metabolic inhibitor sodium azide (3.4 mM) did not significantly influence reaction progress.

Results and Discussion

Reaction of EDTA with CoOOH. *Peak Identification.* An electropherogram collected 8.8 h after addition of excess EDTA to CoOOH at pH 4.6 is presented in Figure 3A. When the benzoate buffer was replaced with an acetate buffer, no additional product peaks were evident. Free EDTA and $Co^{III}EDTA^-$, the product of ligand-assisted dissolution (reaction 2), have been identified with a high degree of certainty: (i) spiking the sample with authentic standards causes these peaks to grow; (ii) the EDTA peak absorbs at 185 nm but not at 254 nm; (iii) the $Co^{III}EDTA^-$ peak absorbs more strongly at 254 nm than at 185 nm, as expected for Co^{III}-containing complexes. The peak at 5.2 min can be assigned to $Co^{II}EDTA^{2-}$ with reasonable certainty, since it coincides with the peak obtained with independently prepared $Co^{II}EDTA^{2-}$ and since it is still apparent when the detection wavelength is switched from 185 to 254 nm. The peak at 5.1 min coincides with the peak obtained with free ED3A and, as expected, does not absorb at 254 nm. Calibration curves have been measured to quantify these four species. It should be noted that the peak assigned to ED3A may coincide with other oxidation products for which authentic standards are not available.

When CoOOH is in excess, two additional peaks appear. A peak at 7.0 min disappears when the detection wavelength is switched from 185 to 254 nm detection, indicating that it is a free aminocarboxylate. It will be referred to as compound "X"; none of our authentic standards (see ref *17*) correspond to this peak. The peak at 11.5 min can be assigned to Co^{III}-$ED3A^0$: (i) spiking the sample with $Co^{III}ED3A^0$ causes this peak to grow; (ii) the compound absorbs more strongly at 254 nm than at 185 nm, indicating that it is a Co^{III}-containing
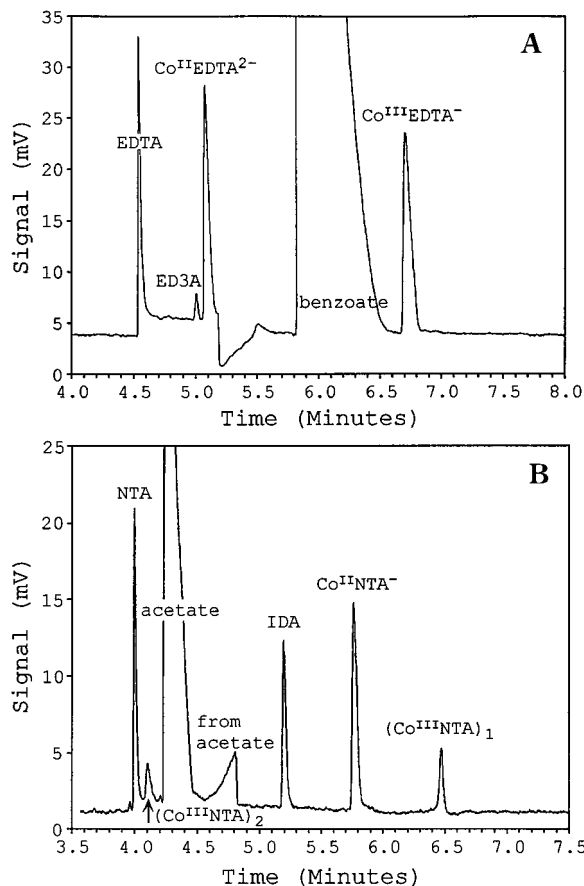

FIGURE 3. CE electropherograms using a detector wavelength of 185 nm. (A) Reaction of 957 μM EDTA with 490 μM CoOOH (pH 4.6, 5.0 mM benzoate buffer, 8.8 h of reaction). (B) Reaction of 983 μM NTA with 537 μM CoOOH (pH 4.9, 5.0 mM acetate buffer, 0.01 M $NaNO_3$ constant ionic medium, 61 h of reaction).

species; (iii) the long electromigration time indicates that the complex is neutral; and (iv) the presence of $ED3A_{free}$ has already been confirmed. In Figure 5, we report peak areas for X and $Co^{III}ED3A^0$, but have not further quantified these peaks.

Product Yield as a Function of Time. As shown in Figure 4, $Co^{III}EDTA^-$ and $Co^{II}EDTA^{2-}$ are the two principal reaction products when 957 μM EDTA is added to 490 μM CoOOH suspensions. As a check for mass balance, the sum ($[EDTA_{free}]$ + $[Co^{III}EDTA^-]$ + $[Co^{II}EDTA^{2-}]$) was plotted as a function of time (not shown). $EDTA_{free}$ is somewhat more difficult to quantify than other free aminocarboxylate species (*17*), and the observed decrease in the sum over the course of the experiment (by less than 60 μM) is close to our experimental uncertainty for this measurement. ED3A was also identified in the reaction solution, but its concentration never exceeded 15 μM.

At pH 4.6, $EDTA_{free}$ drops to half of its original concentration within 10 h. Production of $Co^{III}EDTA^-$ is a little more than double the production of $Co^{II}EDTA^{2-}$ throughout the course of the experiment. At pH 7.3, a longer time is required (approximately 50 h) for $EDTA_{free}$ to again drop to half of its original concentration. Production of $Co^{II}EDTA^{2-}$ is approximately 2 times higher at pH 7.3 than at pH 4.6. Production of $Co^{III}EDTA^-$, however, is approximately half that observed at the lower pH.

The moles of Co^{II} produced in these two reactions is between 3 and 6 times the moles of EDTA consumed, indicating that EDTA serves as a multiple electron reductant toward Co^{III}. With the exception of ED3A, oxidation products
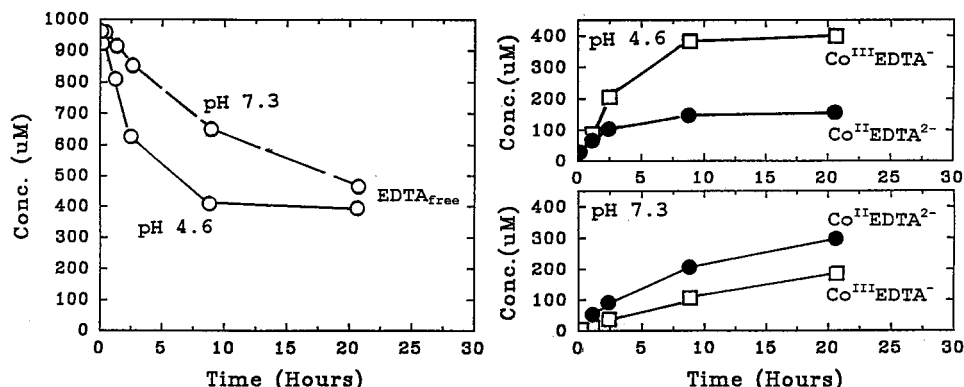
FIGURE 4. EDTA$_{free}$, Co^{II}EDTA^{2-}, and Co^{III}EDTA$^-$ as a function of time during reaction of 957 μM EDTA with 490 μM CoOOH at pH 4.6 (5 mM benzoate buffer) and pH 7.3 (5 mM HEPES buffer).
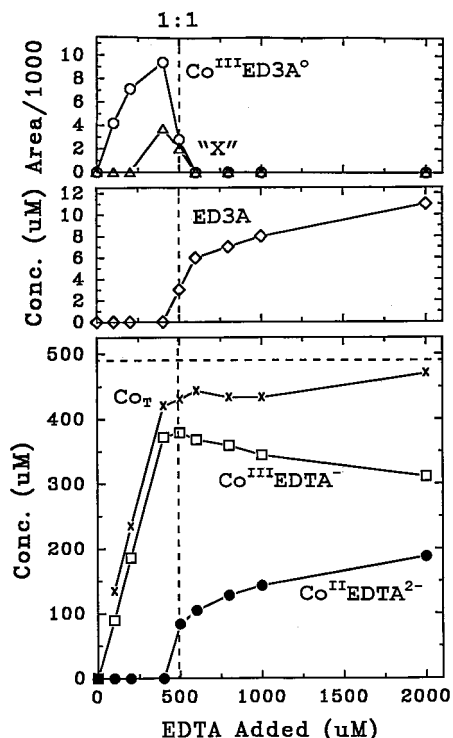

FIGURE 5. Product concentrations (for Co^{II}EDTA^{2-}, Co^{III}EDTA$^-$, Co$_T$, and ED3A$_{free}$) and peak areas (for Co^{III}ED3A^0 and unknown product X) following 30 h of reaction between 490 μM CoOOH and increasing amounts of EDTA at pH 4.6 (5.0 mM benzoate buffer). Co$_T$ represents total dissolved Co measured by AAS. Vertical dashed lines indicate 1:1 stoichiometry between added EDTA and added CoOOH.

were not present in sufficient concentration to allow them to be detected.

The pronounced increase in yield of Co^{II}EDTA^{2-} relative to Co^{III}EDTA$^-$ when the pH is increased from 4.6 and 7.3 is not easy to explain. Although Co^{II} may be retained by the solid during the early portion of the reaction (31), concentrations determined after complete dissolution (e.g., 20 h) accurately reflect the overall reaction stoichiometry. Ligand exchange reactions and electron-transfer reactions between metal centers (reactions 2, 4, 7, 8, and 10) do not change the final yield of Co^{II} and Co^{III}. Reactions resulting in the net oxidation of EDTA (reactions 3, 5, 6, and 11) or analogous reactions of EDTA oxidation products are the only way to increase yields of Co^{II} relative to Co^{III}.

Product Yield as a Function of EDTA Concentration. Figure 5 reports product yields for a series of experiments employing increasing EDTA concentrations at fixed CoOOH loading (at pH 4.6). The 30-h reaction time ensured that CoOOH dissolution was complete. Examining how product concentrations change as a function of EDTA$_{added}$ provides important clues regarding the importance of reactions 1−11 in Figure 2.

We begin with the portion of Figure 5 representing experiments where CoOOH$_{added}$ (490 μM) is in excess relative to EDTA$_{added}$ (100−400 μM). Total dissolved cobalt (Co$_T$) after 30 h of reaction nearly matches EDTA$_{added}$, and 65−90% of Co$_T$ can be attributed to Co^{III}EDTA$^-$. A considerable effort was made to quantify the small amount of Co^{III}ED3A^0 produced. When EDTA$_{added}$ was equal to 400 μM, [Co^{III}ED3A^0] was as high as 45 μM, which nearly completes the mass balance.

The appearance of the oxidation products ED3A (as Co^{III}-ED3A^0) and X indicate that EDTA oxidation has taken place to some extent in experiments where CoOOH$_{added}$ is in excess. The results of a time course experiment performed using 383 μM EDTA and an excess of CoOOH (470 μM) are pertinent here. During the first few hours of reaction, a peak corresponding to Co^{II}EDTA^{2-} is discernible, as well as a larger Co^{III}EDTA$^-$ peak. [Co^{II}EDTA^{2-}] reaches 65 μM after 2.5 h but thereafter decreases until it can no longer be detected. Although Co^{II} may still be present in the system [as Co^{2+}(aq) or as Co$^{II}_{adsorbed}$], it cannot be detected by CE because it is not present as an aminocarboxylate complex. In this time course experiment, Co^{III}ED3A^0 becomes discernible only when the concentration of Co^{II}EDTA^{2-} has begun to decrease.

We can now turn our attention to experiments where EDTA$_{added}$ is in excess. Increasing EDTA$_{added}$ from 500 to 1000 μM results in a substantial drop in [Co^{III}ED3A^0] and a substantial increase in ED3A$_{free}$. These observations are easily explained. Once excess EDTA is available, Co^{III}ED3A^0 is converted to Co^{III}EDTA$^-$ by ligand exchange. Raising EDTA$_{free}$ from 600 to 2000 μM causes an 83% increase in [ED3A$_{free}$] and an 80% increase in [Co^{II}EDTA^{2-}]. [ED3A$_{free}$] is only 6% of [Co^{II}EDTA^{2-}]. Again it is clear that EDTA is a multiple electron reductant for Co^{III} and that a portion of oxidized EDTA goes undetected.

In the range 500 μM < EDTA$_{free}$ < 2000 μM, the sum [Co^{II}EDTA^{2-}] + [Co^{III}EDTA$^-$] equals CoOOH$_{added}$ and Co$_T$ to within analytical uncertainty. As EDTA$_{free}$ is increased, [Co^{II}EDTA^{2-}] grows from 17% to 38% of Co$_T$.

Since EDTA is the ultimate source of reductant capacity in these experiments, it is logical that higher yields of Co^{II}-containing species should accompany increases in EDTA$_{added}$. The appreciable increase in [Co^{II}EDTA^{2-}] once a stoichiometric excess of EDTA has been achieved might indicate that free EDTA (and free EDTA oxidation products) are more readily oxidized than the metal ion-coordinated species. Thus, reactions 3 and 6 appear more important than reactions 5 and 11.

Effect of Cu^{II} and Co^{II} Additions on Product Yield. In one set of experiments, 0, 50, 100, 200, 300, and 400 μM Cu^{II} were added to 1004 μM EDTA solutions prior to addition to suspensions containing 450 μM CoOOH. After 43 h of reaction (4.3 < pH < 4.6, 5 mM benzoate buffer), Cu^{II} additions had no discernible effect on the yields of $Co^{II}EDTA^{2-}$, $Co^{III}EDTA^-$, $[ED3A]_{free}$, and Co_T (data not shown).

In a second set of experiments, comparable concentrations of Co^{II} were added to 1004 μM EDTA solutions prior to its addition to 450 μM CoOOH. The effects on product yield were much more dramatic, however. $[Co^{II}EDTA^{2-}]_{produced}$ was calculated by subtracting Co^{II}_{added} from measurements of $[Co^{II}EDTA^{2-}]$; this quantity decreased from 152 to 40 μM as Co^{II}_{added} was increased from 0 to 400 μM. $[ED3A_{free}]$ decreased from 12.4 to 3.7 μM, and $[Co^{III}EDTA^-]$ increased from 328 to 444 μM.

Even at the maximum concentration added (400 μM), Co^{II} and Cu^{II} are only able to lower $[EDTA_{free}]$ by 40% in the early stages of reaction. We can hypothesize that $Cu^{II}EDTA^{2-}$ is unreactive with the surface; oxidation of the coordinated ligand via reaction 11 is probably not important in Cu^{II} complexes. $Co^{II}EDTA^-$, in contrast, reacts with the surface via reaction 10, thereby generating $Co^{III}EDTA^-$. We hypothesize that Co^{II} additions encourage reaction 10 at the expense of reactions 3 and 6. As a consequence, less EDTA oxidation takes place during the early portions of the reaction. By the time most of the $Co^{II}EDTA^{2-}$ has been oxidized to $Co^{III}EDTA^-$, decreases in $EDTA_{free}$ have slowed reactions 3 and 6 substantially, lessening their influence on the final product yield.

Reaction of NTA with CoOOH. An electropherogram collected 61 h after the addition of excess NTA to CoOOH at pH 4.9 is shown in Figure 3B. Peaks for NTA, $(Co^{II}NTA)_2$, IDA_{free}, $Co^{II}NTA^-$, and $(Co^{III}NTA)_1$ all increase when the appropriate authentic standard is added to the sample. Peaks for $(Co^{III}NTA)_2$ and $(Co^{III}NTA)_1$ absorb more strongly at 254 nm than at 185 nm as expected for Co^{III} complexes, while the other peaks do not.

EDTA possesses log K values for metal ion complex formation that are significantly higher than those for NTA. Shifts in metal ion speciation caused by the addition of EDTA can be used to help identify CE peaks. When EDTA is added to the sample shown in Figure 3B, the $Co^{II}NTA^-$ peak disappears, the NTA_{free} peak grows, and a new peak (corresponding to $Co^{II}EDTA^{2-}$) appears. Over longer periods of time, EDTA addition causes the peak for $(Co^{III}NTA)_1$ to diminish and peaks for NTA_{free} and $Co^{III}EDTA^-$ to grow. Changes to the $(Co^{III}NTA)_2$ peak cannot be seen because its electromigration time is the same as for $EDTA_{free}$.

In the range 4.5 < pH < 5, NTA reacts with CoOOH nearly as fast as EDTA. Dissolution reactions are complete by 15 h, and product yields do not change significantly for at least another 100 h (not shown).

Figure 6 reports product yields for a series of experiments employing increasing NTA concentrations at fixed CoOOH loading (pH 4.9, 61 h of reaction). Because some dissociation of the $Co^{II}NTA^-$ complex during CE analysis occurs (see ref *17*), care must be taken in its quantification. It is quite apparent, however, that concentrations of $Co^{II}NTA^-$ and the ligand oxidation product IDA_{free} are significantly higher and begin at lower ligand concentrations in reactions with NTA relative to analogous reactions with EDTA. Neither Co^{III}-$(IDA)_2^-$ isomer was detected in the NTA experiments. Any Co^{II}-IDA complexes that may have formed are not detectable by CE (*17*).

We did not generate calibration curves for $(Co^{III}NTA)_1$ and $(Co^{III}NTA)_2$. The Co^{III} complexes for which calibration curves were generated ($Co^{III}EDTA^-$, $Co^{III}ED3A^0$, and the two isomers of $Co^{III}(IDA)_2^-$) all yield response factors within 30% of one another. If we apply this response factor to the two
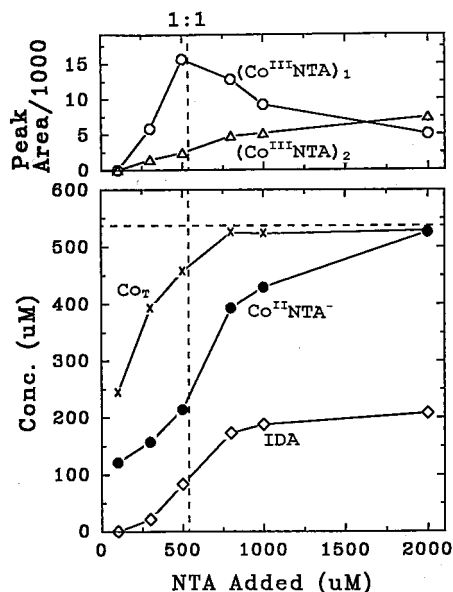

FIGURE 6. Product concentrations for $Co^{II}NTA^-$, Co_T, and IDA_{free} and peak areas for $(Co^{III}NTA)_1$ and $(Co^{III}NTA)_2$ following 61 h of reaction between 537 μM CoOOH and increasing amounts of NTA at pH 4.9. Samples contained 5.0 mM acetate buffer and 0.01 M $NaNO_3$ constant ionic medium. Vertical dashed lines indicate 1:1 stoichiometry between added NTA and added CoOOH.

Co^{III}−NTA complexes, their combined concentrations are of the same magnitude as the discrepancy between Co_T and $[Co^{II}NTA^-]$. It is interesting to note that $[(Co^{III}NTA)_1]$ reaches a maximum value when NTA_{added} and $CoOOH_{added}$ are present in 1:1 stoichiometry. The decrease in $[(Co^{III}NTA)_1]$ once NTA is in excess may arise from (i) a greater yield of $Co^{II}NTA^-$, similar to our findings with EDTA, and (ii) conversion of $(Co^{III}NTA)_1$ into the dimer $(Co^{III}NTA)_2$, favored by higher $[NTA_{free}]$.

Again, evidence for increased reduction of Co^{III} at higher NTA concentrations are reasonable, given that NTA is the ultimate source of reductant capacity in these experiments. The moderate increase in $[Co^{II}NTA^-]$ once a stoichiometric excess of NTA has been achieved provides additional evidence that free aminocarboxylates are oxidized more readily than those coordinated to Co^{III}.

Reactions of IDA with CoOOH. Electropherograms collected after reaction of excess IDA with CoOOH (not shown) reveal the presence of two new peaks corresponding to *u-fac*-$Co^{III}(IDA)_2^-$ and its geometrical isomer *s-fac*-Co^{III}-$(IDA)_2^-$. Amino groups from two IDA molecules are coordinated side-by-side in the *u-fac* isomer but on opposite sides of the central Co^{III} atom in the *s-fac* isomer (*17*). Their identities were confirmed by (i) spiking the sample with authentic standards of both isomers and (ii) demonstration that both peaks absorb more strongly at 254 nm than at 185 nm. The stoichiometry $Co^{III}(IDA)_2^-$ is further supported by the observation that complete CoOOH dissolution only occurs when $[IDA_{added}]$ is at least twice $[CoOOH_{added}]$. No other peaks were discernible.

The experiments reported in Figure 7 employed IDA concentrations that were twice that of $CoOOH_{added}$. Dissolution occurs solely through the ligand-assisted pathway, as indicated by stoichiometric conversion of IDA_{free} into the two $Co^{III}(IDA)_2^-$ isomers, whose combined concentration nearly equals Co_T. Loss of IDA_{free} occurs more slowly at pH 7.3 than at pH 4.6. More than 1 week is required for complete dissolution of CoOOH to occur, far slower than analogous reactions with EDTA and NTA.

At pH 4.6, production of the *u-fac* isomer is more than twice that of the *s-fac* isomer. At pH 7.3, however, the yield
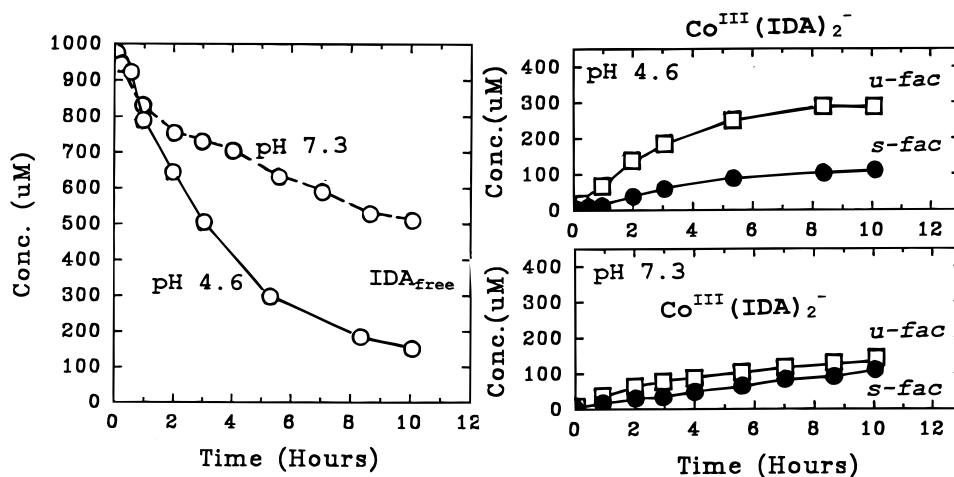
FIGURE 7. IDA$_{free}$, u-fac-Co^{III}(IDA)$_2^-$, and s-fac-Co^{III}(IDA)$_2^-$ as a function of time during reaction of 960 μM IDA with 470 μM CoOOH at pH 4.6 (10 mM acetate buffer) and at pH 7.3 (10 mM HEPES buffer).

of the *u-fac* isomer is only slightly higher than that of the *s-fac* isomer. It is known that rates of isomer interconversion, quite slow under acidic conditions, increase with increasing pH (*32*). Thus, the lower yield of the *u-fac* isomer at pH 7.3 may reflect a greater degree of interconversion.

Reactions of Aminocarboxylate Chelating Agents with MnOOH. Klewicki and Morgan (*33*) recently completed a study of the reaction between EDTA and MnOOH (manganite). In support of their work, we have performed dissolution experiments with four aminocarboxylate chelating agents and used CE to identify and quantify products of the reaction with EDTA.

Dissolution experiments were performed using 1000 μM aminocarboxylate chelating agent and 500 μM MnOOH at pH 7.2 (10 mM MOPS buffer). Initial rates of MnOOH dissolution (dMn_T/dt, in mol L^{-1} s^{-1}) decreased in the order: EDTA (1.6 × 10^{-8}) > HEEDTA (1.1 × 10^{-8}) > NTA (3.7 × 10^{-9}) > IDA (4.6 × 10^{-11}). Mn^{III} complexes absorb strongly in the 400−500 nm range (*34*). Despite this fact, supernatant solutions recovered at the end of each dissolution experiment yielded no discernible absorbance, despite the development of significant Mn_T (total dissolved Mn). Either reductive dissolution dominates reactions with MnOOH or ligand-assisted dissolution is rapidly followed by reduction of dissolved Mn^{III}.

Figure 8 reports on the loss of EDTA$_{free}$ and the appearance of reaction products during reaction of 2000 μM EDTA with 1000 μM MnOOH at pH 5.2. In agreement with UV/visible absorbance measurements, CE analysis fails to provide any evidence for dissolved Mn^{III} complexes. Peaks identified as Mn^{II}EDTA^{2-}, ED3A, and EDDA possessed electromigration times that were the same as authentic standards of each species. A moderate discrepancy (20−30%) between [Mn^{II}-EDTA^{2-}] and Mn_T was observed early in the reaction but dropped to negligible levels after 4 or 5 h of reaction. Mn^{2+}(aq) and complexes that dissociate during electromigration (e.g., Mn^{II}ED3A$^-$ and Mn^{II}EDDA^0) cannot be detected by the CE method we employed.

As a check for mass balance, the sum of all detected aminocarboxylate species ([EDTA$_{free}$] + [Mn^{II}EDTA^{2-}] + [ED3A$_{free}$] + [EDDA$_{free}$]) was calculated. After 24 h, MnOOH dissolution is complete, and the value for this sum is only 71% of EDTA$_{added}$. The remaining 29% of added EDTA has apparently been oxidized to species that are not detected by CE.

Closing Remarks. The ability of EDTA, NTA, and IDA to solubilize mineral surface-bound Co^{III} has been confirmed. The slower solubilization of CoOOH relative to analogous
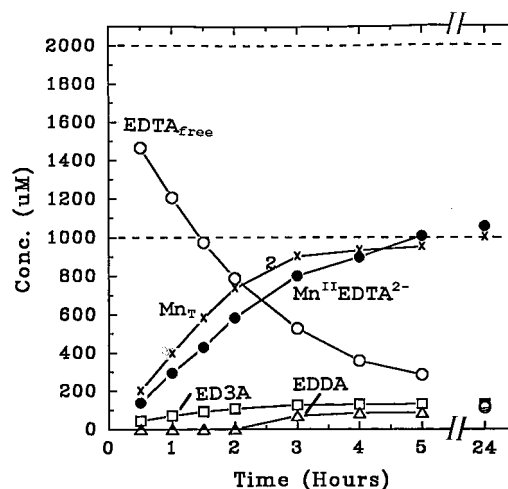

FIGURE 8. EDTA$_{free}$, ED3A$_{free}$, EDDA$_{free}$, Mn^{II}EDTA^{2-}, and Mn_T as a function of time during reaction of 2000 μM EDTA with 1000 μM MnOOH at pH 5.2 (5.0 mM benzoate buffer).

reactions of FeOOH (*35*) is entirely attributable to low rates of Co^{III} ligand exchange.

Given the stability of Co^{III}EDTA$^-$ complexes in solution, CoOOH redox reactions with EDTA and NTA are faster and of greater significance than expected. The reactivity of Co^{III} held within the (hydr)oxide surface may differ in important respects from that of dissolved Co^{III} species. In addition, heterogeneous systems afford pathways for electron transfer (Figure 2) that are not available in homogeneous solution. The observation that EDTA and NTA engage in redox reactions while IDA does not is important. Oxidative conversion of chelating agents to their breakdown products probably lowers the capacity of co-contaminant mixtures to solubilize cobalt. Adsorption/desorption experiments with cobalt−breakdown product complexes must be conducted to confirm this conclusion.

The absence of detectable Mn^{III}−aminocarboxylate complexes is a key finding of our experiments with MnOOH. Mn^{III} is a more facile oxidant than Co^{III} (*31*), hence reactions analogous to reactions 3, 5, 10, and 11 (Figure 2) are faster for MnOOH than for CoOOH. Free multidentate chelating agents (e.g., EDTA, NTA) apparently do not persist in the presence of MnOOH. Hence, reaction with manganese (hydr)oxides may represent a sink for aminocarboxylates comparable in magnitude to biodegradation (*36−40*).

Literature Cited

(1) Means, J. L.; Alexander, C. A. *Nucl. Chem. Waste Manage.* **1981**, *2*, 183−196.

(2) Killey, R. W.; McHugh, J. O.; Champ, D. R.; Cooper, E. L.; Young, J. L. *Environ. Sci. Technol.* **1984**, *18*, 148−157.

(3) Olsen, C. R.; Lowry, P. D.; Lee, S. Y.; Larsen, I. L.; Cutshall, N. H. *Geochim. Cosmochim. Acta* **1986**, *50*, 593−607.

(4) Means, J. L.; Crerar, D. A.; Duguid, J. O. *Science* **1978**, *200*, 1477−1481.

(5) Girvin, D. C.; Gassman, P. L.; Bolton, H., Jr. *Soil Sci. Soc. Am. J.* **1993**, *57*, 47−57.

(6) Zachara, J. M.; Gassman, P. L.; Smith, S. C.; Taylor, D. *Geochim. Cosmochim. Acta* **1995**, *59*, 4449−4463.

(7) Zachara, J. M.; Smith, S. C.; Kuzel, L. S. *Geochim. Cosmochim. Acta* **1995**, *59*, 4825−4844.

(8) Jardine, P. M.; Taylor, D. L. *Geochim. Cosmochim. Acta* **1995**, *59*, 4193−4203.

(9) Brooks, S. C.; Taylor, D. L.; Jardine, P. M. *Geochim. Cosmochim. Acta* **1996**, *60*, 1899−1908.

(10) Murray, J. W.; Dillard, J. G. *Geochim. Cosmochim. Acta* **1979**, *43*, 781−787.

(11) Crowther, D. L.; Dillard, J. G.; Murray, J. W. *Geochim. Cosmochim. Acta* **1983**, *47*, 1399−1403.

(12) Dillard, J. G.; Schenck, C. V. In *Geochemical Processes at Mineral Surfaces*; Davis, J. A., Hayes, K. F., Eds.; ACS Symposium Series 323; American Chemical Society: Washington, DC, 1986; pp 503−522.

(13) Hem, J. D.; Roberson, C. E.; Lind, C. J. *Geochim. Cosmochim. Acta* **1985**, *49*, 801−810.

(14) Bricker, O. *Am. Mineral.* **1965**, *50*, 1296−1354.

(15) Robie, R. A.; Heingway, B. S.; Fisher, J. R. *Thermodynamic Properties of Minerals and Related Substances at 298.1 K and 1 Bar (10^5 Pascals) Pressure and at Higher Pressures*; Geological Survey Bulletin 1452; USGS: Washington, DC, 1978.

(16) Klewicki, J. K.; Morgan, J. J. *Environ. Sci. Technol.* **1998**, *32*, 2916−2922.

(17) Bürgisser, C. S.; Stone, A. T. *Environ. Sci. Technol.* **1997**, *31*, 2656−2664.

(18) Ogino, H.; Shimura, M. *Adv. Inorg. Bioinorg. Mech.* **1986**, *4*, 107−135.

(19) Hamm, R. E.; Suwyn, M. A. *Inorg. Chem.* **1967**, *6*, 139−145.

(20) Gangopadhyay, S.; Ali, M.; Saha, S. K.; Banerjee, P. *J. Chem. Soc., Dalton Trans.* **1991**, 2729−2734.

(21) Yashiro, M.; Mori, T.; Yoshikawa, S.; Shiraish, S. *Chem. Lett.* **1993**, *6*, 1009−1012.

(22) Rodrigues, M.-C.; Lambert, F.; Morgenstern-Badarau, I.; Cesario, M.; Guilhem, J.; Keita, B.; Nadjo, L. *Inorg. Chem.* **1997**, *36*, 3525−3531.

(23) Dwyer, F. P.; Gyarfas, E. C.; Mellor, D. P. *J. Phys. Chem.* **1955**, *59*, 296−297.

(24) Hidaka, J.; Shimura, Y.; Tsuchida, R. *Bull. Chem. Soc. Jpn.* **1962**, *35*, 567−571.

(25) Mori, M.; Shibata, M.; Kyuno, E.; Okubo, Y. *Bull. Chem. Soc. Jpn.* **1958**, *31*, 940−944.

(26) Hey, M. H. *Mineral. Mag.* **1962**, *33*, 253−259.

(27) Deliens, M.; Goethals, H. *Mineral. Mag.* **1973**, *39*, 152−157.

(28) Giovanoli, R.; Leuenberger, U. *Helv. Chim. Acta* **1969**, 2333−2347.

(29) Skoog, D. A.; West, D. M. *Fundamentals of Analytical Chemistry*; Holt, Rinehart & Winston: New York, 1976.

(30) Feitknecht, W.; Marti, W. *Helv. Chim. Acta* **1945**, *28*, 145−156 (as cited in ref *14*).

(31) Stone, A. T.; Ulrich, H.-J. *J. Colloid Interface Sci.* **1989**, *132*, 509−522.

(32) Kawaguchi, H.; Ama, T.; Yasui, T. *Bull. Chem. Soc. Jpn.* **1984**, *57*, 2422−2427.

(33) Klewicki, J. K. Ph.D. Thesis, California Institute of Technology, Pasadena, CA, 1996.

(34) Davies, G. *Coord. Chem. Rev.* **1969**, *4*, 199−224.

(35) Nowack, B.; Sigg, L. *Geochim. Cosmochim. Acta* **1997**, *61*, 951−963.

(36) Tiedje, J. M. *J. Appl. Microbiol.* **1975**, *30*, 327−329.

(37) Madsen, E. L.; Alexander, M. *Appl. Environ. Microbiol.* **1985**, *50*, 342−349.

(38) Lauff, J. J.; Steele, D. B.; Coogan, L. A.; Breitfeller, J. M. *Appl. Environ. Microbiol.* **1990**, *56*, 3346−3353.

(39) Bolton, H.; Girvin, D. C.; Plymale, A. E.; Harvey, S. D.; Workman, D. J. *Environ. Sci. Technol.* **1996**, *30*, 931−938.

(40) Bolton, H.; Girvin, D. C. *Environ. Sci. Technol.* **1996**, *30*, 2057−2065.